DRUG DELIVERY
2020, VOL. 27, NO. 1, 652–661
https://doi.org/10.1080/10717544.2020.1756984

Taylor & Francis
Taylor & Francis Group

ORIGINAL PAPER

Incorporation of ion exchange functionalized-montmorillonite into solid lipid nanoparticles with low irritation enhances drug bioavailability for glaucoma treatment

Shuo Liu[a], Xinyue Han[a], Hanyu Liu[a], Yawen Zhao[a], Huamei Li[a], Ilva D. Rupenthal[b], Zhufen Lv[c], Yanzhong Chen[c], Fan Yang[c], Qineng Ping[d], Yufang Pan[a] and Dongzhi Hou[a]

[a]College of Pharmacy, Guangdong Pharmaceutical University, Guangzhou, PR China; [b]Buchanan Ocular Therapeutics Unit, Department of Ophthalmology, New Zealand National Eye Center, Faculty of Medical and Health Sciences, University of Auckland, Auckland, New Zealand; [c]Guangdong Engineering and Technology Research Center of Topical Precise Drug Delivery System, College of Pharmacy, Department of Pharmaceutics, Guangdong Pharmaceutical University, Guangzhou, PR China; [d]College of Pharmacy, China Pharmaceutical University, Nanjing, PR China

ABSTRACT

Montmorillonite-loaded solid lipid nanoparticles with good biocompatibility, using Betaxolol hydrochloride as model drug, were prepared by the melt-emulsion sonication and low temperature-solidification methods and drug bioavailability was significantly improved in this paper for the first time to application to the eye. The appropriate physical characteristics were showed, such as the mean particle size, Zeta potential, osmotic pressure, pH values, entrapping efficiency (EE%) and drug content (DC%), all showed well suited for possible ocular application. *In vitro* release experiment indicated that this novel system could continuously release 57.83% drugs within 12 h owing to the dual drug controlled-release effect that was achieved by ion-exchange feature of montmorillonite and structure of solid lipid nanoparticles. Low irritability and good compatibility of nanoparticles were proved by both CAM-TBS test and cytotoxicity experiment. We first discovered from the results of Rose Bengal experiment that the hydrophilicity of the drug-loaded nanoparticles surface was increased during the loading and releasing of the hydrophilic drug, which could contribute to prolong the ocular surface retention time of drug in the biological interface membrane of tear-film/cornea. The results of *in vivo* pharmacokinetic and pharmacodynamics studies further confirmed that increased hydrophilicity of nanoparticles surface help to improve the bioavailability of the drug and reduce intraocular pressure during administration. The results suggested this novel drug delivery system could be potentially used as an in situ drug controlled-release system for ophthalmic delivery to enhance the bioavailability and efficacy.

ARTICLE HISTORY
Received 12 March 2020
Revised 13 April 2020
Accepted 14 April 2020

KEYWORDS
Solid lipid nanoparticles (SLNs); Betaxolol hydrochloride (BH); montmorillonite (Mt); immortalized human cornea epithelial cells (iHCECs); intraocular pressure (IOP)

1. Introduction

Glaucoma is a group of diseases characterized by atrophy and depression of the optic nipples, visual field defects, and decreased vision (Cohen & Pasquale, 2014). Pathologically elevated intraocular pressure (IOP) of the optic nerve is the primary risk factor for the glaucoma (Weinreb & Khaw, 2004). Reducing IOP is an effective treatment for glaucoma. Conventional methods for the treatment of glaucoma include medical therapies and surgical therapies (Cohen & Pasquale, 2014). Medical therapies refer to application of the drugs with an effect of reducing IOP on the eye in the form of certain preparations, such as prostaglandin analogs (Tang et al., 2019), β-blockers (Xu et al., 2017), α-agonists (Arthur & Cantor, 2011) and carbonic anhydrase inhibitors (Kalinin et al., 2019). Betaxolol hydrochloride (BH), as a selective β-adrenergic blocker, can prominently lower IOP and has been widely used in the treatment of glaucoma for its advantages of less systemic toxic and side effects (Erkin et al., 2006; Huang et al., 2016).

The eye, an independent and sensitive organ of the human body, has multiple anatomic and physiologic characteristics (Agarwal et al., 2016; Leonardi et al., 2015; Park et al., 2015), such as lachrymal drainage, tear turnover (Yavuz & Kompella, 2017) and inherent protective barriers: the cornea-conjunctiva barriers, the blood-retinal barrier (Yellepeddi et al., 2015) which effectively prevent the invasion of potentially microorganisms and toxins, meanwhile great challenges are also rose for delivering effective dose drug to the intended site of action to achieve considerable therapeutic level. Currently, for most eye diseases of the anterior segment, topical instillation of traditional ophthalmic preparations (e.g., topical eye drops) is the most attractive and conventional route of treatment (Imperiale et al., 2018).

CONTACT Yufang Pan p39352353@126.com; Dongzhi Hou houdongzhi406@163.com College of Pharmacy, Guangdong Pharmaceutical University, No. 280, Outer Ring Road, Guangzhou Higher Education Mega center, Guangzhou 510006, China

However, owing to the limitations above, the drug bioavailability of traditional ophthalmic preparations is limited, thus the compliance of patients becomes poor due to the increase of dosing frequency for chronic disease of glaucoma. Data also showed that only a few small portion of drug (<5%) could be absorbed by effective channel (Joseph & Venkatraman, 2017; Shen et al., 2018). In order to improve the drug bioavailability, many nano-scale drug delivery systems were created.

Nano-scale drug delivery systems (nanocapsules, nanoparticles, liposomes, nanoemulsion, etc.) show significant therapeutic advantages in the field of ophthalmic therapy, such as increased pre-corneal retention time, sustained drug release and targeted delivery to specific eye tissue (Chetoni et al., 2015). Among those nano-scale drug delivery systems, solid lipid nanoparticles (SLNs) with nano-sized particles (100–700 nm) not only possess most superior characteristics already mentioned above, but also could avoid the common disadvantages found in other nano-systems, such as limited physical stability, cytotoxicity of polymers and the leakage of drugs encapsulated, etc. (Baig et al., 2016; Chetoni et al., 2016). SLNs are composed of low toxic physiological and biodegradable lipids from natural or synthetic sources. Furthermore, its solid core could prevent the particles from coalescing (Chen & Foldvari, 2016) and drastically reduce the mobility of incorporated drug molecules in a solid phase, which diminished leakage of the drug from the carriers (Seyfoddin et al., 2010). Therefore, SLNs are regarded as a potential candidate for ophthalmic delivery systems (Hao et al., 2011) .

In this paper, BH which belongs to water-soluble cation drug was selected as the model drug. In order to control the release of BH for the treatment of chronic disease of glaucoma, SLNs were selected as drug controlled release carrier. To further improve sustained-release performance of SLNs, montmorillonite (Mt) was selected as constitutive materials for its great potential as a controlled-release delivery vehicle of therapeutic agents in the pharmaceutical field (Alboofetileh et al., 2013; dos Santos et al., 2015) in this study. Mt belongs to smectite group clays, which are also known as phyllosilicates that consist of silica tetrahedral sheets layered between alumina octahedral sheets (Santos et al., 2015; Hou et al., 2016). The flexibility of interlayer spacing of layered silicates could control the rate of drug releasing from drug-intercalated layered materials and help drug to be replaced with the inorganic exchangeable cations (Lin et al., 2009). Similarly, Wang et al. (2008) reported that the release of bovine serum albumin (BSA) from N-(2-hydroxyl) propyl-3-trimethylammonium chitosan chloride (HTCC)/montmorillonite complex could be lowered compared to pure compound owing to the application of Mt. Thus, drug intercalated Mt could be used as a quality controlled-release drug delivery system.

In our present study, a novel delivery system of Mt-BH-SLNs was invented by the combination of SLNs and Mt-BH complex to investigate and modulate the performance of drug release (Hou et al., 2003). BH molecules were intercalated into Mt interlayer spacing to form Mt-BH complex and further the complex were entrapped into SLNs to form novel ion-exchange ocular delivery system of Mt-BH-SLNs, thus the dual controlled-release effect of drug was achieved. The physical-chemical characterizations of Mt-BH-SLNs were evaluated, such as pH values, osmotic pressure, mean particle size and size distribution, Zeta potential, morphology, entrapping efficiency (EE%), drug content (DC%), stability and *in vitro* release curve. Cytotoxicity test on human immortalized cornea epithelial cells (iHCECs) and chorioallantoic membrane-trypan blue staining assay (CAM-TBS) were both implemented to evaluate potential irritation of formulation. Rose Bengal assay, *in vivo* ocular pharmacokinetics and pharmacodynamics studies were conducted, respectively, to evaluate the influence of surface hydrophobicity of the SLNs on prolonging residence time of drug on ocular surface, improving drug bioavailability and the effect of lowing IOP. These studies will pave the way for developing better topic ophthalmic drug delivery systems for glaucoma treatment.

2. Materials and methods

2.1. Chemicals and animals

BH was purchased from Jinan Haohua industrial (Shandong, China). Mt was obtained from Aladdin (Shanghai, China). Glycerin monostearate (GMS) was purchased from Aladdin Industrial Corporation. Phosphatidylcholine (PC) was obtained from Taiwei pharmaceutical (Shanghai, China). Rose Bengal was purchased from Macklin (Shanghai, China). Dulbecco's Modified Eagle Media: Nutrient Mixture F-12(DMEM/F-12) and Penicillin were purchased from Hyclone (Beijing, China), Fetal bovine serum was obtained from Gbico (Paisley, UK). 1-(4,5-dimethylthiazol-2-yl)-3,5-diphenylformazan (MTT) and all components of buffer solution were from Sigma (Shanghai, China). All other chemical reagents used in the study were of HPLC or analytical grade.

All *in vivo* experiments were carried out in New Zealand white rabbits (2.5-3.0 kg) obtained from the Laboratory Animal Center of Southern Medical University, Guangzhou, China (License No:SCXK2012-2015). All the animals were treated according to the Association for Research in Vision and ophthalmology resolution for the use of animals in research and were approved by the Institutional Animal Care and Use Committee of Guangdong pharmaceutical university (approval number of the animal experiment protocols is gdpulac2019010). Before the experiment, animals were ensured without eye diseases.

2.2. Preparation of Mt-BH-SLNs

Based on our previous studies, Mt was first acidified in 5% H_2SO_4 for 0.5 h at 70 °C to obtain acidified Mt (Acid-Mt) with increased special surface area and cation exchange capacity, and then BH was intercalated into intercalate spacing of Acid-Mt to form Mt-BH complex by solution intercalation (Hou et al., 2015; Huang et al., 2017). The SLNs were prepared via the melt-emulsion sonication and low temperature-solidification methods (Figure 1; Lee et al., 2007).

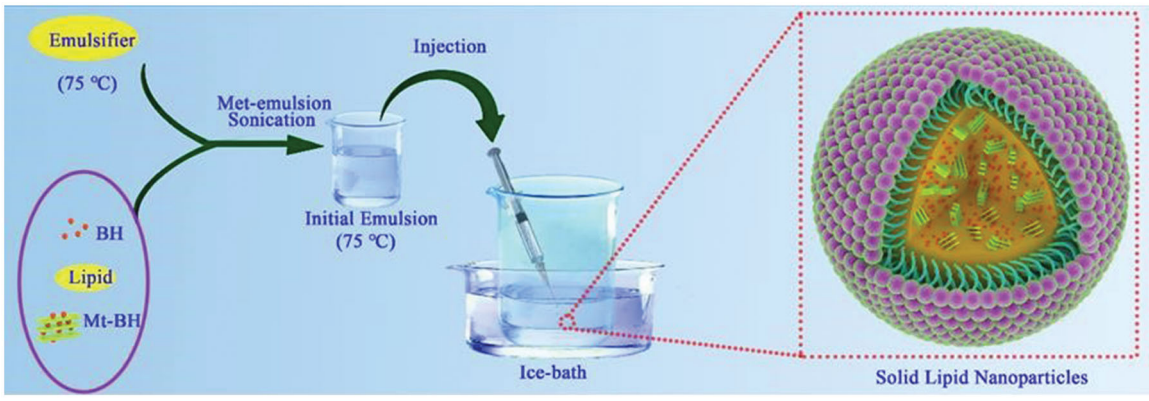

Figure 1. The schematic illustration for the formation of Mt-BH-SLNs. Initial emulsion was obtained by subjecting organic phase containing the emulsifier and the internal aqueous phase containing Mt-BH with met-emulsion sonication. Solid lipid nanoparticles were prepared by injecting the initial emulsion into external aqueous phase with rapid stirring in an ice-water bath.

In brief, BH, GMS and PC (ratio = 1:1:3) were dissolved into 5 mL of ethyl alcohol by heating at 75 °C, as the organic phase. Subsequently, 5 mg of Mt-BH complex was added to the organic phase and then sonicated (JY92-II Ultrasound Cell Disintegrator, Shanghai Xiren Instrument Co., Ltd) for 5 min in ice-water bath. The resultant mixture was maintained at 75 °C and slowly injected into 2 g·L^{-1} preheated aqueous surfactant solution that contained Tween 80, PEG-400 and sodium deoxycholate (ratio = 40:20:1) under magnetic stirring (RCT Magnetic Stirrer, IKA Company, Germany) at 800 rpm and then an initial emulsion was obtained. In order to yield a uniformly dispersed formulation and solidify SLNs, the initial emulsion was quickly injected into external aqueous phase (0 °C) of 3.6% mannitol (osmotic medium) in ice-water bath and stirred at 1000 rpm for 2 h. Blank-SLNs (without BH) were prepared in a similar way.

2.3. Characterization of Mt-BH-SLNs

2.3.1. Osmotic pressure and pH values measurement

An osmometer (Osmomat Basic 3000, GonotecGmBTH, Germany) was used to evaluate osmotic pressure of Mt-BH-SLNs. The pH values of Mt-BH-SLNs was detected by a pH meter (PHS-3C, INESA Scientific Instrument Co., Ltd). All the measurements were applied in triplicate at room temperature.

2.3.2. Particle size, zeta potential and morphology

The average particle size and Zeta potential of Mt-BH-SLNs were determined using dynamic light scattering and electrophoretic light scattering (Beckman apparatus, Coulter, USA), respectively. The samples were appropriately diluted with deionized water. Morphological evaluation of the SLNs was performed using transmission electron microscopy (TEM) technique by negative staining method. A drop of the sample was applied to a film-coated copper grid and stained with 2.0% phosphotungstic acid after the sample was completely dry. The particles in grids were observed under a transmission electron microscope (Philips TECNAI10, Holland) at an acceleration voltage of 115 kV (Mou et al., 2019).

2.3.3. Entrapping efficiency (EE%) and drug content (DC%)

Dynamic dialysis method was selected to measure entrapping efficiency (EE%) and drug content (DC%) of Mt-BH-SLNs (Jain et al., 2014). Tightened dialysis bags (8000-14000 MWCO, Sigma) containing 4 mL samples were immersed into 30 mL phosphate buffered saline (PBS) to be incubated for 45 min at 120 rpm and 34 °C ± 0.5 °C. Three parallel trials were performed. The BH amount of each group was quantified with UV spectrophotometry (UV-1800; Shanghai mapada Instruments Co., Ltd, China) at 273 nm (maximum absorbance wavelength for BH in PBS medium) after filtering by 0.22 μm syringe filter (Purifying Equipment Manufacturing, Shanghai, China). A full dose was obtained by dissolving the samples into 10 mL methanol under ultrasound treatment and measuring by UV spectrophotometry. EE% and DC% were calculated according to the following equations (Fernandes et al., 2020):

$$EE\% = \frac{Total\ Drug\ Contant\ (mg) - Free\ Drug\ Contant\ (mg)}{Total\ Drug\ Contant\ (mg)} \times 100$$

$$DC\% = \frac{Actual\ Drug\ Contant\ (mg)}{Theoretical\ Drug\ Contant\ (mg)} \times 100$$

2.3.4. Stability study

The short-term storage stability study of SLNs was conducted for one month to investigate the effect of storage temperature (Hou et al., 2003). The batch was divided into two portions and stored in transparent colorless glass vials under different temperature conditions of 4 °C (in a refrigerator) and 25 °C (at room temperature). Initial particle size, polydispersity index (PDI), Zeta potential and the appearance of the SLNs dispersion were measured. A part of samples was withdrawn after 10th day, 20th day and 30th day and evaluation indicators mentioned above were determined again to evaluate the stability.

2.3.5. In vitro *release study*

In vitro release of BH from BH solution and Mt-BH-SLNs dispersion was determined by membrane dialysis method (Onyebuchi & Kavaz, 2019) and freshly prepared simulated tear fluid (STF) (NaCl 0.678 g, $NaHCO_3$ 0.218 g, $CaCl_2 \cdot 2H_2O$ 0.0084 g, KCl 0.138 g and deionized water 100 mL) was selected as release medium. Generally, 2 mL samples were dropped into the dialysis bags (8000-14000 Da), which could intercept Mt-BH-SLNs diffusion and allow the diffusion of free drug molecules into release medium, and immersed in 30 mL STF, then the system was shaken in water-bath at 120 rpm, 34 °C. The release medium (5 mL) was withdrawn at predetermined time intervals within 12 h and immediately replaced with an equal volume and temperature of STF to maintain a constant volume. The amount of samples was analyzed by the HPLC method (Agilent Instrument 1200, USA) with a Shimadzu column (250 × 4.60 mm). A mixture of acetonitrile and 0.05% triethylamine (3:7, V/V) was used as mobile phase. The detector flow rate, wavelength, and column temperature was 1 mL·min^{-1}, 273 nm and 30 °C, respectively.

2.4. Irritation evaluation

2.4.1. CAM-TBS test

The CAM-TBS test can not only visually observe the irritation of the preparations but also quantitatively analyze results, and reduce the use of experimental animals (do Nascimento et al., 2012). Therefore CAM-TBS test was selected to investigate ocular tolerability of the formulations. Briefly, the shell and the inner membranes of 10-day-old fertilized eggs were carefully removed to expose chorioallantoic membrane (CAM) without damage. During the study, a loop with an 18-mm diameter was added on the surface of CAM to limit the scope of administration. Then, 300 μL of formulations (BH solution, Blank-SLNs and Mt-BH-SLNs) were instilled directly onto the CAM surface in loop, respectively, and contacted for 5 min. Then the CAM surface was washed with saline and stained with 0.5 mL trypan blue solution (TBS, 1 mg·mL^{-1}) for 1 min. TBS was a cell dye that dyed dead cells to light blue. Subsequently, the dyed CAM was excised and the adsorbed trypan blue was extracted with 1 mL formamide overnight. Finally, the extract of trypan blue was determined by UV (UV-1800; Shanghai mapada Instruments Co., Ltd, China) at 611 nm.

2.4.2. Cytotoxicity test

The human immortalized cornea epithelial cells (iHCECs) were cultured in Dulbecco's Modified Eagle Media: Nutrient Mixture F-12 (DMEM/F-12) media supplemented with 10% (v/v) heat-inactivated fetal bovine serum, 0.1 mg·mL^{-1} streptomycin and penicillin (Chen et al., 2018). The survival rate of iHCECs after exposure of formulations was determined by MTT test (Angius & Floris, 2015). The iHCECs (1 × 104 cells) were seeded in 96-well microplates. Then the cells were exposed to different amount of BH solution, Blank-SLNs and Mt-BH SLNs for 120 min. Following the exposure, the culture medium containing MTT was added to the cells and incubated for 4 h at 37 °C. MTT (3-(4,5-dimethyl-2-thiazolyl)-2,5-diphenyl-2-H-tetrazolium bromide) only could act on the respiratory chain in the mitochondria of living cells, and then the tetrazolium ring of MTT was cracked under the action of succinate dehydrogenase and cytochrome C to form blue insolubility formazan crystals. Subsequently, the MTT solution was removed and the formazan was dissolved by DMSO. The absorbance was measured by microplate reader (Thermo Fisher Scientific, USA) at 570 nm.

2.5. In vivo *experiment*

2.5.1. Surface hydrophobicity evaluation

Rose Bengal (RB; disodium 2, 3, 4, 5-tetrachloro-6-(2,4,5,7-tetraiodo-3-oxido-6-oxoxanthen-9-yl) experiment (Doktorovova et al., 2012) was performed to analyze the surface hydrophobicity of Mt-BH-SLNs, Acid-Mt-SLNs and BH aqueous solution. RB is hydrophobic and can be combined with nanoparticle surface hydrophobic groups. Briefly, samples from 1 mL to 10 mL were added to corresponding twice volume of RB aqueous solution with fixed concentration of 0.03 mg·mL^{-1}, respectively. All the mixture was incubated at room temperature (25 °C) in the dark for 3 h. Free RB moleculesmolecule, which did not bound to the particle surface, was separate from SLNs by centrifugation for 30 min at 15000 rpm and its content (RB_{free}) was detected with UV spectrophotometry at 549 nm. Free RB solution should be filtered by 0.22 μm syringe filters before UV spectrophotometry to avoid the influence of unsettled nanoparticles and impurities in the supernatant. Alternatively, K, the binding constant of evaluating particle surface hydrophobicity, was be calculated according to Scatchard equation:

$$\frac{r}{a} = \mathrm{KN} - \mathrm{Kr}$$

Where r is the concentration of bound RB ($[RB_{bound}] = [\mathrm{RB}] - [RB_{free}]$, [RB] is the total concentration of RB), a is the equilibrium concentration of RB, K is the binding constant and N is the maximal amounts of bound RB.

2.5.2. In vivo *pharmacokinetic study in aqueous humor*

Pharmacokinetic study in the aqueous humor was carried out using micro-dialysis (MD) technique (Cremers et al., 2012). Ocular MD is a biochemical sampling technology that continuously monitors the dynamic changes of extracellular fluid substances (including endogenous and exogenous substances) in living eyes (Kamata 2003). Briefly, rabbits were randomly divided into BH solution groups and Mt-BH-SLNs groups. Rabbits in all groups were treated with ofloxacin ophthalmic solution for 3 days before surgery to prevent ocular inflammation. A micro-dialysis probe (BASI, USA) was implanted into the anterior chamber of each eye as described in Figure 4(c), after the animals were anesthetized with pentobarbital sodium injection. Subsequently, the wound surfaces were treated with two drops of ofloxacin ophthalmic solution and the rabbits were placed into

restrainers with permitted free movement of the head for one-day recovery to obtain filled aqueous humor. Before the administration of formulations, the equilibration period was obtained by priming the microdialysis probes with saline solution for 1.5 h. Then the eyes were treated with 100 μL of formulations. Immediately, the dialysate was collected continuously every 30 min for 6 h. Drug concentration in aqueous humor was analyzed via HPLC (Agilent Instrument 1200, USA) with a Shimadzu column (250 × 4.60 mm). *In vivo* recovery was calculated by following formula:

$$R = (C_{in} - C_{out})/(C_m - C_{out})$$

Where C_{in} is the concentration of standard solutions, C_{out} is the concentration of dialysate, C_m is the concentration in aqueous humor.

2.5.3. In vivo *pharmacodynamics study*

New Zealand white rabbits were selected as experimental animals. The IOP of each rabbit's eyes was monitored daily by an indentation tonometer (YZ7A, Suzhou Visual Technology Co. Ltd., China) and only those animals with constant pressure were selected for study. The animals were randomly divided into two groups, the BH group and the Mt-BH-SLNs group, to evaluate the effect of lowering IOP of formulations. After anesthesia, acute high intraocular pressure models were induced by intraperitoneal injection of saline (Tian et al., 2018). The IOP of every modeled eye was determined instantly as the initial IOP when the animals woke up. Subsequently, the right eye was treated with formulations and the left eye was given saline as a control. IOP was measured at regular time intervals after ocular application of eye drops and saline. All measurements under the same environmental condition were evaluated by the same operator.

2.6 Statistical analyses

Date were represented as mean values ± SD (standard deviation) and statistically assessed by one-way analysis of variance (ANOVA). P value less than 0.05 was assumed for the statistically significant differences.

3. Results and discussion

3.1. Preparation and physical characterization of Mt-BH-SLNs

Melted lipids of hot homogenization and internal aqueous phase containing Tween-80 as the emulsifier were used to prepare initial emulsion (W/O). Then SLNs (W/O/W) dispersion was formed by injecting the initial emulsion (W/O) into external aqueous phase and solidified by continuous stirring in ice-bath. The appearance of resulted SLNs was clear with a pale blue opalescence, and the Tyndall effect was irradiated by the beam (Figure 2(b)).

The osmotic pressure and pH values of Mt-BH-SLNs were 276 ± 7 mOsm·L^{-1} and 6.88 ± 0.30, respectively, which both met the requirements of ophthalmic preparations. The produced Mt-BH-SLNs system showed spherical morphology (Figure 2(a)), Zeta potential of 20.145 ± 0.005 mV ($n = 3$) and the average diameter of 149.5 ± 2.2 nm ($n = 3$) with a narrow PDI values of 0.285 ± 0.045 ($n = 3$), which could avoid the patients discomforts and eye irritate response such as blinking and production of tear caused by large size (>10 μm). In addition, the positive charge on the surface of particle is beneficial for adhering to the negatively charged corneal epithelium and causing repulsion between particles to prevent aggregation and ultimate to maintain samples stability. The considerable size, narrow PDI and the positive charge of SLNs promoted the increasing of ocular surface retention time allowing drug molecules to be sustained released from the nanoparticles, thereby improving drug bioavailability. The higher encapsulation efficiency (EE%) and the drug contant (DC%) of Mt-BH-SLNs were showed as 79.27 ± 3.31% and 101.33 ± 0.90%, respectively.

3.2. Physical stability study

While the particle size of SLNs was enough small to apply in the eyes, them still suspended in solvent for Brown movement. Temperature is a critical factor for Brown movement of particles and the rise of temperature was directly proportional to severity of Brownian movement, which could cause the lack of particles stability. Therefore, physical stability study was carried out to find appropriate storage temperate. The changes of mean particle size, PDI and Zeta potential were used as the prime parameters to evaluate the stability of the formulations. In general, the mean particle size of formulation stored at 25 °C was slightly increased from 149.5 nm to 210.3 nm ($p < .05$) at the 30th day. Whereas, for samples stored at 4 °C, mean particle diameter, Zeta potential and PDI all had no significant alterations ($p > .05$) in 30 days. In addition, the appearance was still translucent, with a light blue opalescence. Due to the fact that relative high temperature (25 °C) increased the kinetic energy of system and so the degree of Brown movement was increased which could accelerate the collision of particles, and consequently increasing the possibility of aggregation for nanoparticles (Lee et al., 2007). Conclusively, the Mt-BH-SLNs were relatively stable at the storage temperature of 4 °C (Table 1).

Both particle diameter and PDI of formulation stored at 25 °C significantly changed but there was no obvious change at 4 °C, indicating that mean particle diameter of SLNs increased with increasing storage temperature. Values are presented as the mean ± SD ($n = 3$).

3.3. In vitro *release study*

In vitro drug release study is important to understand and predict the *in vivo* performance of the dosage form. Figure 2(c) depicts the *in vitro* release curves of BH from Mt-BH-SLNs and BH solution. We observed that BH rapidly was released from the BH solution in the initial 30 min and completely released within 2 h. And the accumulative amounts of BH released from Mt-BH-SLNs were about 46.70% at 2 h and only 57.83% until 12 h.

The *in vitro* release curve of Mt-BH-SLNs shows a certain degree of burst effect in about 1 h because the free drug

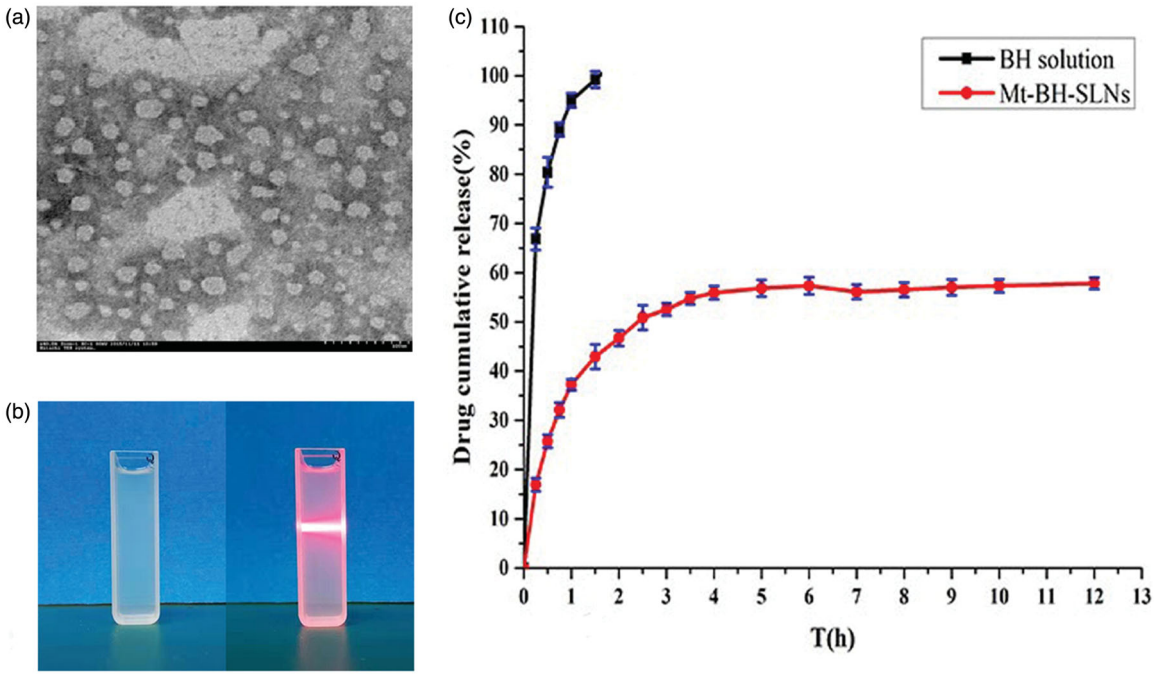

Figure 2. (a) The TEM of the Mt-BH-SLNs; (b) The appearance of Mt-BH-SLNs; (c) *In vitro* release of BH from Mt-BH-SLNs and BH solution. Studies performed in freshly prepared simulated tear fluid (STF) at 34 °C. Values are presented as the mean ± SD ($n = 3$).

Table 1. The stability of Mt-BH-SLNs at 4 °C and 25 °C ($n = 3$).

	4 °C			25 °C		
Time (d)	Particle size (nm)	Zeta (mV)	PDI	Particle size (nm)	Zeta (mV)	PDI
0	149.5 ± 3.2	18.24 ± 1.2	0.185 ± 0.017	149.5 ± 2.2	18.14 ± 1.2	0.285 ± 0.045
10	152.2 ± 2.1	18.01 ± 0.4	0.182 ± 0.014	167.2 ± 1.1	17.01 ± 0.4	0.282 ± 0.033
20	151.5 ± 1.5	17.74 ± 1.7	0.186 ± 0.011	181.5 ± 1.2	16.04 ± 1.7	0.296 ± 0.026
30	150.3 ± 0.8	19.04 ± 0.9	0.184 ± 0.009	210.3 ± 2.8	17.17 ± 0.9	0.284 ± 0.015

molecules were adsorbed onto the surface of nanoparticles during the cooling preparation procedure. Then an obvious slower release of BH from Mt-BH-SLNs was showed which may attribute to the ion-exchange property of Mt and the solid lipid nanoparticles structure. The BH molecules incorporated in Mt layer were released by ion-exchange interaction with cation ions in the STF. *In vitro* release curve of Mt-BH-SLNs was fitted to different kinetic equations such as Zero order, First order, Higuchi, Hixcon Crowell, Ritger-Peppas, Weibull and Korsmeyer-Peppas equations (Table 2; Chatterjee et al., 2011; Kumar et al., 2013). The First order equation ($r^2 = 0.989$) and Korsmeyer-Peppas ($r^2 = 0.9876$) equation fitted the curve well, which were better kinetic modules ($r^2 = 0.9876$). Meanwhile, the release index ($n = 0.6641$) of Mt-BH SLNs could be obtained from the result of Mt-BH SLNs *in vitro* release curve fitting Korsmeyer-Peppas equation. The *n* value of Mt-BH SLNs is between 0.45 and 0.89, indicating that the release of BH molecules in SLN is mainly non-Fick diffusion. So the release mechanism of Mt-BH-SLNs was synergy of diffusion and corrosion.

3.4. Irritation evaluation

3.4.1. CAM-TBS test

Figure 3(a) exhibits the CAM-TBS results of formulations. It was clearly seen that irritation of each formulation was in the sequence: BH solution > Mt-BH-SLNs > Blank-SLNs. The trypan blue absorption of the Blank-SLNs was greater than that of the Mt-BH-SLNs, which may be due to the irritation caused by BH. However, the irritation of drug was significantly reduced for Mt-BH-SLNs compared to BH solution. In addition, after the instillation of Mt-BH-SLNs and Blank-SLNs to CAM, no remarkable irritating symptoms (e.g., hemolysis) were showed. This suggested that the irritation of the drug could be reduced by loading the drug into Mt and further formed SLNs.

An ideal carrier system for ophthalmic application should have good ocular tolerability (Araujo et al., 2009). In this study, the potential irritancy of compounds was evaluated by a quantitative analysis method that measured the UV absorption of trypan blue after exposure to chemicals (CAM-TBS) (M A Fathalla et al., 2017). Trypan blue is a cell reactive dye, which is commonly used to detect the integrity of the cell membrane to further distinguish live cells and dead cells (Louis & Siegel, 2011). Vinardell & García (2000) had demonstrated that the absorbed amount of trypan blue was proportional to the irritation.

SLNs, composed of biocompatible lipid material, could incorporate free BH molecules to release drug at a slow rate. Damage caused by high topical drug concentration could be avoided without burst release effect. These results revealed that BH was incorporate into Mt and eventually formed Mt-BH-SLNs, which could improve safety compared with BH solution.

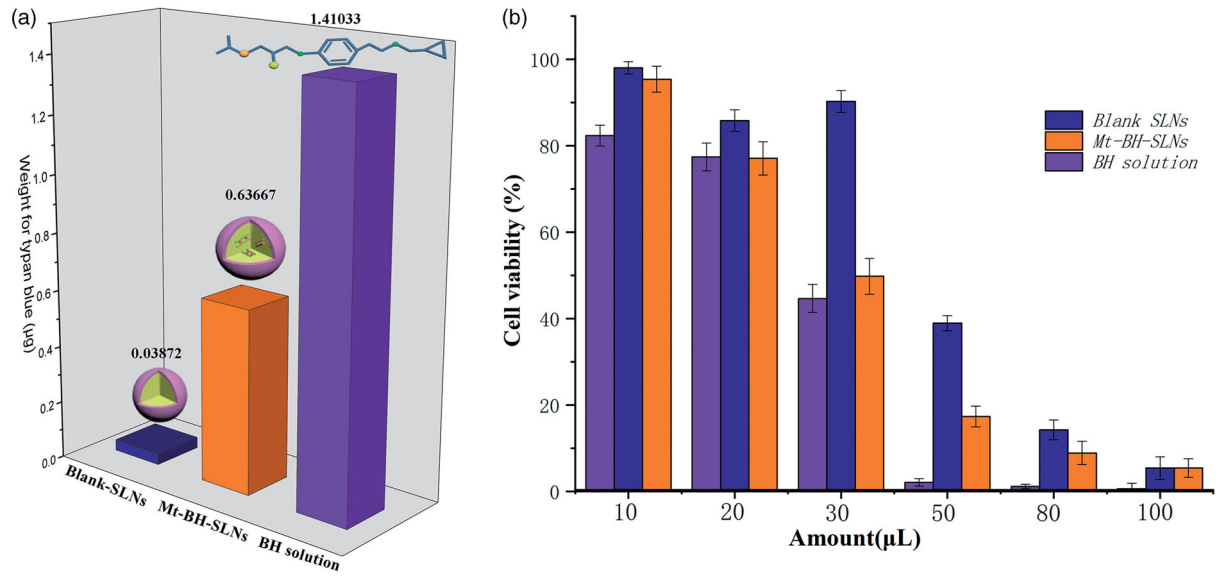

Figure 3. (a) The absorption of trypan blue after exposure to formulations (Blank-SLNs, Mt-BH-SLNs and BH solution); (b) The viability of cells being exposed to different amount of BH solution, Mt-BH-SLNs and Blank-SLNs for 120 min. Values are presented as the mean ± SD ($n = 3$).

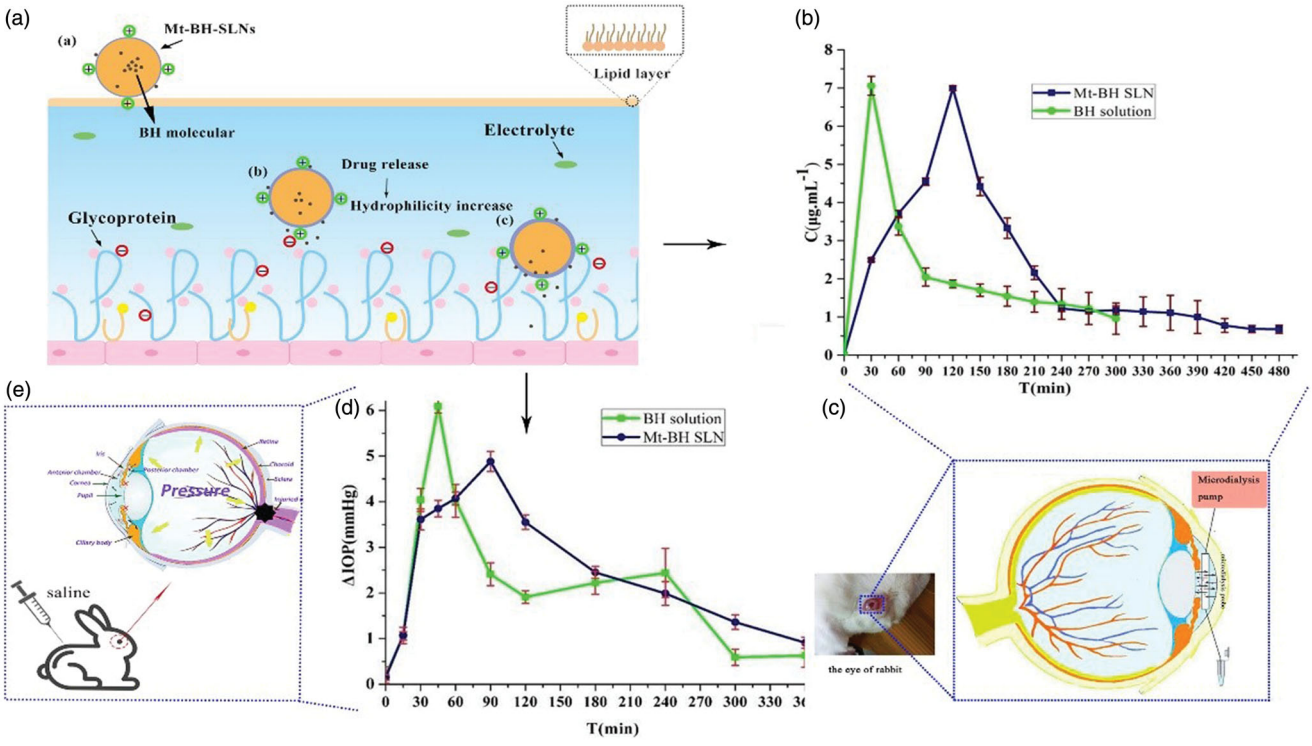

Figure 4. (a) The process of interaction between Mt-BH-SLNs and mucin in ocular tear film. Tear film was composed of lipid layer, aqueous layer and mucin layer. Mt-BH-SLNs with opposite charge to mucin bind to it by electrostatic interaction. The hydrophilicity of Mt-BH-SLNs surface was improved due to the release of water-soluble BH to the nanoparticles surface. Mt-BH-SLNs with increased surface hydrophilicity could penetrate or dissolve in aqueous mucus, and ocular surface retention time could be prolonged; (b) Concentration of BH in rabbit aqueous humor at various time points after instillation of different formulations; (c) The microdialysis sampling technique of rabbit eye; (d) The pharmacological response (the decrease in IOP, △IOP) versus time profiles for BH solution and Mt-BH-SLNs; (e) The schematic drawing of IOP, which caused by blocked aqueous circulation and further damaged the optic nerve head.

3.4.2. Cytotoxicity test

The viability of cells being exposed to different amount of BH solution, Mt-BH-SLNs and Blank-SLNs for 120 min was shown in Figure 3(b). No remarkable difference in the cell viability of BH solution, Blank-SLNs and Mt-BH-SLNs was exhibited after application of 10 μL and 20 μL. BH solution and Mt-BH-SLNs both showed significant ($p < .05$) cytotoxicity and the cell viability decreased to 44.65% and 49.79%, respectively, when the amount of formulations increased to 30 μL. Meanwhile, the cell viability of Blank-SLNs was

Table 2. Mathematical models of regression for *in vitro* release profiles of Mt-BH-SLNs.

	Mt-BH-SLNs		BH solution	
	Equation	r^2	Equation	r^2
Zero order	$Y = 3.2649t + 31.4810$	0.487	$Y = 39.1331t + 42.7317$	0.512
First order	$\ln(100\text{-}Y) = -1.0712t + 4.0319$	0.989	$\ln(100\text{-}Y) = -3.9281t + 4.5899$	0.986
Higuchi	$Y = 16.21t^{1/2} + 8.287$	0.916	$Y = 34.80\sqrt{t} + 49.66$	0.972
Weibull	$\ln \ln[100/100\text{-}Y] = 0.5514t + 4.1441$	0.975	$\ln \ln [100/100\text{-}Y] = 0.5232t + 4.7034$	0.999
Hixson-Crowell	$(100\text{-}Y)^{1/3} = -0.078t + 4.243$	0.828	$\sqrt[3]{(100\text{-}Y)} = -2.249t + 4.428$	0.989
Ritger-Pappas	$\log Y = 0.2218\log t + 1.5689$	0.838	$\log Y = 0.2009\log t + 1.9637$	0.962
Korsmeyer-Peppas	$Y = 52.401t^{0.6641}$	0.9876	$Y = 84.328t^{0.6188}$	0.9976

approximately 90.26%, so the carrier of SLNs itself was very low toxicity and was a safer carrier choice. Higher cytotoxicity was shown and the cell viability of BH solution decreased to 2.07% when applied formulation of 50 μL. We could find that model drug BH itself was relatively cytotoxic, but its inclusion in SLN could effectively reduce cytotoxicity, especially in the high concentration range. In addition, considering that the cytotoxicity of BH was so serious, improving the encapsulation efficiency of SLN was necessary. This was consistent with the results of the CAM-TBS test.

According to the results of EE% and DC%, a part of BH molecules were not encapsulated in SLNs and were presented on the surface of SLNs or were free in solvent, so that Mt-BH-SLNs showed higher toxicity in comparison to Blank-SLNs. However, cytotoxicity of Mt-BH-SLNs was weaker than that of BH solution, so the toxicity of BH could be reduced by being encapsulated into Mt and SLN. Based on data above our findings, we concluded that SLNs as an ocular carrier could reduce the irritation caused by drug.

3.5. In vivo *experiment*

3.5.1. *Surface hydrophobicity evaluation*

Ocular mucin with hydrophilic properties and rich negative charges is the main component of the tear film, which benefits to stabilize the tear film, wet the cornea, and prevent the invasion of pathogens (Georgiev et al., 2019; Read et al., 2019). Meanwhile, it also prevent the effective dose of the drug from reaching the target tissue (Hori 2018). The binding constant values (K) of Acid-Mt-SLNs, Blank-SLNs and Mt-BH-SLNs were determined to analyze and evaluate the surface hydrophobicity properties of SLNs during application. The data in Table 3 show that the K value of Mt-BH-SLNs is the smallest, which means that the hydrophobicity of Mt-BH-SLNs is the weakest among Acid-Mt-SLNs, Blank-SLNs and Mt-BH-SLNs. There is almost no significant difference in K values between Acid-SLNs and Blank-SLNs. The results could be attributed to the impact of the excess free BH molecules which did not capsulated into SLNs in the suspension, dissolution of excess free BH molecules deposited on the surface of SLNs while cooling during preparation and the slowly release of a part of BH molecules to the surface of Mt-BH-SLNs when nanoparticles were incubated with the RB aqueous solution for a while in the RB experiment, leading to the improvement of Mt-BH-SLNs surface hydrophilicity.

Therefore, when administered, the positively charged Mt-BH-SLNs would first bind to the negatively charged corneal mucin. Meanwhile, BH was continuously released from Mt-BH-SLNs and gradually the hydrophilicity of Mt-BH-SLNs was increased. It was beneficial to dissolve in or pass through the mucin layer, deliver more doses of drugs to the site of action, prolong the residence time of nanoparticles in the corneal epithelium and improve drug bioavailability. This prediction was validated in the following *in vivo* pharmacokinetic and pharmacodynamics analysis.

Table 3. Scatchard-plot equation and Rose Bengal binding constant values (K) of Mt-BH-SLNs, Acid-Mt-SLNs and Blank-SLNs.

Types of SLN	Scatchard-plot equation	K values
Mt-BH-SLNs	$y = -75.206x + 2.008$	75
Acid-Mt-SLNs	$y = -87.06x + 2.2438$	87
Blank-SLNs	$y = -88.159x + 2.3465$	88

Table 4. Pharmacokinetic parameters of BH in rabbit aqueous humor after instillation of different formulations.

Pharmacokinetic parameters	AUC_{0-t} (μg/mL·min)	T_{max} (h)	C_{max} (μg/mL)	MRT_{0-t} (h)
Mt-BH-SLNs	1086.96	2	6.99	2.841
BH solution	660.48	0.5	7.05	1.849

3.5.2. *Pharmacokinetic study in aqueous humor*

The BH concentration in the aqueous humor versus time after topical administration of BH solution and Mt-BH-SLNs were shown in Figure 4(b). BH solution was immediately absorbed into the aqueous humor to reach maximum concentration (C_{max}) at 0.5 h and drug concentration remarkably decreased in the following hours. Finally, BH concentration in the aqueous humor was not detectable after 300 min. In contrast, the concentration of BH in the aqueous humor increased slowly after instillation of Mt-BH-SLNs and reached a peak at 2 h, and then gradually decreased for 480 min. The pharmacokinetic parameters for BH in the aqueous humor are summarized in Table 4. The data clearly indicate that Mt-BH-SLNs produced higher T_{max} (4-fold) ($p < .05$), MRT_{0-t} (1.53-fold) ($p < .05$) and AUC (1.64-fold) ($p < .05$) than BH solution.

After the concentration of BH solution and Mt-BH-SLNs in the aqueous humor reaching C_{max}, significant downward trends were observed both of them, which were caused by the loss of the drug in the conjunctival sac and the tear wash. However, the decline curve of BH concentration in Mt-BH-SLNs was gentle compared to that of BH solution due to the slow release controlled by Mt and SLN. The results confirmed the former in vitro release experiment.

Mt-BH-SLNs had a longer MRT than that of BH solution, indicating that Mt-BH-SLNs could greatly prolong the pre-

corneal residence time due to adhesion effect caused by increased hydrophilicity of nanoparticle surface, which facilitated drugs penetration into aqueous humor further to improve drug bioavailability (Lin et al., 2014).

3.5.3. In vivo *pharmacodynamics study*

In this study, rabbit model of experimental glaucoma (Figure 4(e)) was applied to evaluate the ability of lowering-IOP of samples. The basal IOP was about 15 mmHg and the high IOP rabbit models could maintain high IOP within 300 min and then returned to baseline value. Thus, the experiment should be over in 6 h. Figure 4(d) shows the ΔIOP versus follow-up time after high IOP rabbit models being administrated formulations. For BH solution, the sharp peak IOP-lowering effect (4.04 mmHg) was obtained in 30 min and then the IOP-lowering effect rapidly decreased. An upward trend of ΔIOP still was shown in 120 min and a sharp decline in 240 min. The IOP-lowering ability of BH solution was unstable. It might be attributed to the rapid permeability of BH itself because BH molecules are small enough to pass through the mucus network (Gipson et al., 2004) and the ΔIOP decreased almost simultaneously due to the weak adhesion ability of BH molecules being cleared away quickly by blinking, tears turnover, etc.

The pharmacodynamics curve Mt-BH-SLNs could be observed that ΔIOP in the first 30 min was almost similar to that of BH solution. This is because a part of BH was not wrapped in SLNs and suspended in formulations solution in the form of free molecules. Mt-BH-SLNs continuously lowered IOP and achieved strongest IOP-lowering effect (4.88 mmHg) in 90 min. Subsequently a sustained and stable downward trend of IOP was followed. Although the ΔIOP of Mt-BH-SLNs was almost the same to that of BH solution in 6 h, a downward trend could be forecasted in the curve of Mt-BH-SLNs and a gentle trend was found in the curve of BH solution after 6 h. This implied that the IOP-lowering effect of Mt-BH-SLNs would be continued for more than 6 h in a stable form.

This could be attributed to that SLNs provided better tissue adherence due to its positive charge, biocompatibility and surface hydrophobicity changes, allowing more of the drug to diffuse into the intraocular target site. Hence, Mt-BH-SLNs showed effective therapeutic effect for glaucoma and maintained a relatively steady IOP-lowering effect.

For glaucoma, a chronic disease, the application of Mt-BH-SLNs could continuously and steadily release drug of effective dose to improve treatment effect and reduce dosing frequency to further improve patient compliance.

4. Conclusion

In this study, a novel ocular delivery system of Mt-BH-SLNs with appropriated osmotic pressure, pH values, mean particle size, PDI, Zeta potential, EE% and DC% was prepared by the melt-emulsion sonication and low temperature-solidification method. Sustained drug release of Mt-BH-SLNs was shown by *in vitro* release study. The results of CAM-TBS test and cytotoxicity test both revealed greater corneal biocompatibility of Mt-BH-SLNs compared to BH solution. The results of Rose Bengal study, *In vivo* pharmacokinetics and pharmacodynamics study showed the increased hydrophilicity of SLNs during drug administration contributed to prolong pre-corneal retention time and further to improve the ability of reducing IOP. The present study suggested the potential effectiveness of Mt-inserted SLNs with dual controlled-release for glaucoma treatment.

Acknowledgments

Guangdong Provincial Engineering Center of Topical Precise Drug Delivery System is acknowledged for their help in performing the experiments.

Disclosure statement

The authors report no conflicts of interest.

Funding

The authors acknowledge financial support from the National Natural Science Foundation of China [NO.51192052] and Science and Technology Planning Project of Guangdong Province [NO.2017B030314175].

References

Agarwal R, Iezhitsa I, Agarwal P, et al. (2016). Liposomes in topical ophthalmic drug delivery: an update. Drug Deliv 23:1–91.

Alboofetileh M, Rezaei M, Hosseini H, et al. (2013). Effect of montmorillonite clay and biopolymer concentration on the physical and mechanical properties of alginate nanocomposite films. J Food Eng 117: 26–33.

Angius F, Floris A. (2015). Liposomes and MTT cell viability assay: an incompatible affair. Toxicol in Vitro 29:314–9.

Araujo J, et al. (2009). Nanomedicines for ocular NSAIDs: safety on drug delivery. Nanomedicine 5:394–401.

Arthur S, Cantor LB. (2011). Update on the role of alpha-agonists in glaucoma management. Exp Eye Res 93:271–83.

Baig MS, Ahad A, Aslam M, et al. (2016). Application of Box-Behnken design for preparation of levofloxacin-loaded stearic acid solid lipid nanoparticles for ocular delivery: optimization, in vitro release, ocular tolerance, and antibacterial activity. Int J Biol Macromol 85:258–70.

Chatterjee A, Kumar L, Bhowmik BB, et al. (2011). Microparticulated anti-HIV vaginal gel: in vitro-in vivo drug release and vaginal irritation study. Pharm Dev Technol 16:466–73.

Chen DW, Foldvari M. (2016). In vitro bioassay model for screening non-viral neurotrophic factor gene delivery systems for glaucoma treatment. Drug Deliv and Transl Res 6:676–85.

Chen X, Sullivan DA, Sullivan AG, et al. (2018). Toxicity of cosmetic preservatives on human ocular surface and adnexal cells. Exp Eye Res 170:188–97.

Chetoni P, Burgalassi S, Monti D, et al. (2016). Solid lipid nanoparticles as promising tool for intraocular tobramycin delivery: Pharmacokinetic studies on rabbits. Eur J Pharm Biopharm 109:214–23.

Chetoni P, Monti D, Tampucci S, et al. (2015). Liposomes as a potential ocular delivery system of distamycin A. Int J Pharm 492:120–6.

Cohen LP, Pasquale LR. (2014). Clinical characteristics and current treatment of glaucoma. Cold Spring Harb Perspect Med 4:a017236.

Cremers TIFH, Flik G, Hofland C, et al. (2012). Microdialysis evaluation of clozapine and N-desmethylclozapine pharmacokinetics in rat brain. Drug Metab Dispos 40:1909–16.

Doktorovova S, Shegokar R, Martins-Lopes P, et al. (2012). Modified Rose Bengal assay for surface hydrophobicity evaluation of cationic solid lipid nanoparticles (cSLN). Eur J Pharm Sci 45:606–12.

Erkin EF, Çelik P, Kayıkçıoğlu Ö, et al. (2006). Effects of latanoprost and betaxolol on cardiovascular and respiratory status of newly diagnosed glaucoma patients. Ophthalmologica 220:332–7.

Fernandes AV, Pydi CR, Verma R, et al. (2020). Design, preparation and in vitro characterizations of fluconazole loaded nanostructured lipid carriers. Braz. J. Pharm. Sci 56:e18069

Georgiev GA, Eftimov P, and Yokoi N, et al. (2019). Contribution of Mucins towards the physical properties of the tear film: a modern update. Int J Mol Sci 20:6132.

Gipson IK, Hori Y, Argüeso P, et al. (2004). Character of ocular surface mucins and their alteration in dry eye disease. The Ocular Surface 2: 131–48.

Hao J, Fang X, Zhou Y, et al. (2011). Development and optimization of solid lipid nanoparticle formulation for ophthalmic delivery of chloramphenicol using a Box-Behnken design. Int J Nanomedicine 6: 683–92.

Hori Y. (2018). Secreted mucins on the ocular surface. Invest Ophthalmol Vis Sci 59:DES151–DES156.

Hou D, Gui R, Hu S, et al. (2015). Preparation and characterization of novel drug-inserted-montmorillonite chitosan carriers for ocular drug delivery. ANP 04:70–84.

Hou D, Hu S, Huang Y, et al. (2016). Preparation and in vitro study of lipid nanoparticles encapsulating drug loaded montmorillonite for ocular delivery. Appl Clay Sci 119:277–83.

Hou D, Xie C, Huang K, et al. (2003). The production and characteristics of solid lipid nanoparticles (SLNs). Biomaterials 24:1781–5.

Huang W, Zhang N, Hua H, et al. (2016). Preparation, pharmacokinetics and pharmacodynamics of ophthalmic thermosensitive in situ hydrogel of betaxolol hydrochloride. Biomed Pharmacother 83:107–13.

Huang Y, Tao Q, Hou D, et al. (2017). A novel ion-exchange carrier based upon liposome-encapsulated montmorillonite for ophthalmic delivery of betaxolol hydrochloride. IJN Volume 12:1731–45.

Imperiale JC, Acosta GB, Sosnik A, et al. (2018). Polymer-based carriers for ophthalmic drug delivery. J Control Release 285:106–41.

Jain AK, Jain A, Garg NK, et al. (2014). Adapalene loaded solid lipid nanoparticles gel: an effective approach for acne treatment. Colloids Surf B Biointerfaces 121:222–9.

Joseph RR, Venkatraman SS. (2017). Drug delivery to the eye: what benefits do nanocarriers offer? Nanomedicine 12:683–702.

Kalinin S, Valtari A, Ruponen M, et al. (2019). Highly hydrophilic 1,3-oxazol-5-yl benzenesulfonamide inhibitors of carbonic anhydrase II for reduction of glaucoma-related intraocular pressure. Bioorg Med Chem 27:115086.

Kamata K. (2003). Effect of a selective inducible nitric oxide synthase inhibitor on intraocular nitric oxide production in endotoxin-induced uveitis rabbits: in vivo intraocular microdialysis study. Pharmacol Res 47:485–91.

Kumar L, Reddy MS, Shirodkar RK, et al. (2013). Preparation and characterisation of fluconazole vaginal films for the treatment of vaginal candidiasis. Indian J Pharm Sci 75:585–90.

Lee M-K, Lim S-J, Kim C-K, et al. (2007). Preparation, characterization and in vitro cytotoxicity of paclitaxel-loaded sterically stabilized solid lipid nanoparticles. Biomaterials 28:2137–46.

Leonardi A, Bucolo C, Drago F, et al. (2015). Cationic solid lipid nanoparticles enhance ocular hypotensive effect of melatonin in rabbit. Int J Pharm 478:180–6.

Lin J, Wu H, Wang Y, et al. (2014). Preparation and ocular pharmacokinetics of hyaluronan acid-modified mucoadhesive liposomes. Drug Deliv 23:1–51.

Lin R-Y, Chen B-S, Chen G-L, et al. (2009). Preparation of porous PMMA/Na+–montmorillonite cation-exchange membranes for cationic dye adsorption. J Membr Sci 326:117–29.

Louis KS, Siegel AC. (2011). Cell viability analysis using trypan blue: manual and automated methods. Methods Mol Biol 740:7–12.

M A Fathalla Z, Vangala A, Longman M, et al. (2017). Poloxamer-based thermoresponsive ketorolac tromethamine in situ gel preparations: design, characterisation, toxicity and transcorneal permeation studies. Eur J Pharm Biopharm 114:119–34.

Mou J, Liu Z, Liu J, et al. (2019). Hydrogel containing minocycline and zinc oxide-loaded serum albumin nanopartical for periodontitis application: preparation, characterization and evaluation. Drug Deliv 26: 179–87.

Nascimento D. F d, Silva AC, Mansur CRE, et al. (2012). Characterization and evaluation of poly(epsilon-caprolactone) nanoparticles containing 2-ethylhexyl-p-methoxycinnamate, octocrylene, and benzophenone-3 in anti-solar preparations. j Nanosci Nanotechnol 12:7155–66.

Onyebuchi C, Kavaz D. (2019). Chitosan and N, N, N-Trimethyl chitosan nanoparticle encapsulation of ocimum gratissimum essential oil: optimised synthesis. IJN 14:7707–27.

Park CG, Kim YK, Kim MJ, et al. (2015). Mucoadhesive microparticles with a nanostructured surface for enhanced bioavailability of glaucoma drug. J Control Release 220:180–8.

Read ML, Navascues-Cornago M, Keirb N, et al. (2019). The impact of contact lens wear on ocular surface mucins using a novel clinical fluorescence imaging system. Cont Lens Anterior Eye S1367-0484: 30224–3.

Santos B. R d, Bacalhau FB, Pereira T. d S, et al. (2015). Chitosan-Montmorillonite microspheres: A sustainable fertilizer delivery system. Carbohydr Polym 127:340–6.

Seyfoddin A, Shaw J, Al-Kassas R, et al. (2010). Solid lipid nanoparticles for ocular drug delivery. Drug Deliv 17:467–89.

Shen J, Lu GW, Hughes P, et al. (2018). Targeted ocular drug delivery with pharmacokinetic/pharmacodynamic considerations. Pharm Res 35:217.

Tang W, Zhang F, Liu K, et al. (2019). Efficacy and safety of prostaglandin analogues in primary open-angle glaucoma or ocular hypertension patients: a meta-analysis. Medicine 98:e16597.

Tian S, Li J, Tao Q, et al. (2018). Controlled drug delivery for glaucoma therapy using montmorillonite/Eudragit microspheres as an ion-exchange carrier. IJN 13:415–28.

Vinardell MP, García L. (2000). The quantitive chlorioallantoic membrane test using trypan blue stain to predict the eye irritancy of liquid scintillation cocktails. Toxicology in Vitro: An International Journal Published in Association with BIBRA 14:551–5.

Wang X, Du Y, Luo J, et al. (2008). Biopolymer/montmorillonite nanocomposite: preparation, drug-controlled release property and cytotoxicity. Nanotechnology 19:065707.

Weinreb RN, Khaw PT. (2004). Primary open-angle glaucoma. The Lancet 363:1711–20.

Xu K, et al. (2017). Impact of combination glaucoma therapies on beta-blocker exposure. J Glaucoma 26:e107–e109.

Yavuz B, Kompella UB. (2017). Ocular drug delivery. Handb Exp Pharmacol 242:57–93.

Yellepeddi VK, Sheshala R, McMillan H, et al. (2015). Punctal plug: a medical device to treat dry eye syndrome and for sustained drug delivery to the eye. Drug Discov Today 20:884–9.